Bifurcation of droplet flows within capillaries

Fabien Jousse
Unilever Corporate Research, Colworth House, Sharnbrook MK44 1LQ, United Kingdom

Robert Farr
Unilever Food & Health Research Institute, 3133AT Vlaardingen, The Netherlands

Darren R. Link
Raindance Technologies, Inc., Guilford, Connecticut 06437, USA

Michael J. Fuerstman
Department of Chemistry and Chemical Biology, Harvard University, 12 Oxford Street, Massachusetts 02138, USA

Piotr Garstecki
Institute of Physical Chemistry, Polish Academy of Sciences, Kasprzaka 44/52, 01-224 Warsaw, Poland
(Received 20 April 2005; revised manuscript received 19 July 2006; published 29 September 2006)

Flows of droplets through networks of microchannels differ significantly from the flow of simple fluids. Our report focuses on the paths of individual droplets through the simplest possible network: a channel that splits into two arms that subsequently recombine. This simple system exhibits complex patterns of flow: both periodic and irregular, depending on the frequency at which the drops are fed into the "loop." A numerical model explains these results and shows regions of regular patterns separated by regions of high complexity. Our results elicit new questions regarding the dynamics of flow of discrete elements of fluids through networks, and point to potential opportunities and difficulties in the design of integrated mini-laboratories operating on droplets.

DOI: 10.1103/PhysRevE.74.036311 PACS number(s): 47.60.+i

I. INTRODUCTION

Microfluidic flows are typically characterized by low values of the Reynolds number [1]. The flow of simple fluids can be described by the linear (Stokes) equations of motion. This linear nature of the flow results in simple flow patterns and facile control of microfluidic systems due to the high robustness of viscous flows to small perturbations. Co flows of immiscible phases introduce intrinsically nonlinear interfacial forces. Surprisingly, two phase flows in confined microgeometries demonstrate the controllability observed in flows of simple fluids. Thus, microfluidic systems offer methods of emulsification [2–4] that are specific to confined geometries and are highly reproducible. Also the flow of drops and slugs through capillaries introduce only weak nonlinearities into the relation between the pressure drop and the speed of flow [5–7].

The introduction of bifurcations and loops into the network of microfluidic channels changes the flow behavior dramatically [3,8,9]. A droplet arriving at a T intersection, if it does not break [3], flows into the branch characterized by lower resistance to flow. Since the presence of slugs in microchannels increases the resistance to flow in the duct [5–7], there is a feedback between choices of successive droplets. This feedback combined with the amplification of a slight difference in resistances of the two diverging branches to a left/right choice of the trajectory make for complicated dynamics. Here, we describe the features of these dynamics in a *microscopic* view: focusing on the trajectories of individual droplets, and not on the statistical properties of flow [9]. This approach opens new questions in the physics of flow of discrete objects through networks, and is relevant to the rapidly expanding field of lab-on-chip devices operating on droplets [10–12].

Flow of dispersions through networks of capillaries is ubiquitous in nature as well as in man-made systems. Examples include flow of blood (dispersion of cells) [13–15], flow of crude oil and water within porous media and rock fractures [16,17], and flow in membrane and bioreactors [18]. In nature, multiphase flows usually occur in large arrays of microducts, while man-made microfluidic devices are typically simple and consist of single-channel modules. Microfluidic devices offer a convenient means for the design of chips to perform multiple tasks in parallel [19–24]. For droplet-based assays—where the ultimate goal is to form, process, and analyze each droplet individually—an essential prerequisite for successful design is a detailed knowledge of the trajectories that the droplets follow at bifurcations. As we demonstrate in this paper, this is not a trivial issue, as many parameters influence the trajectories of droplets. In particular, the viscous dissipation introduced by the drops alters the distribution of pressures in the network of capillaries and the path undertaken by any drop depends on the positions of all the other droplets in the network. While it is possible to steer the droplets actively (using electro-, and dielectrophoresis, surface-acoustic waves, or electrowetting [25,26]), the motion of drops is always associated with a passive response of the system–and thus the effects described in this paper always have to be taken into account. Microfluidic networks also provide a useful model of natural flows in capillaries [27] and studies similar to ours may lead to insights into the dynamics of those complicated, natural, systems.

Here, we report the results of experiments and a numeric study of the simplest network (a loop): a single channel that splits into two arms that subsequently recombine. This simple system has been used recently [8] in a design of a micromixer. Similar loop designs have been studied computationally in the context of hematocrit flows in capillary networks [13–15]. These studies show that dynamical effects modulate cell distribution in a loop [13] and can lead to chaotic time distribution series [14], both effects reproduced with our simple model.

II. RESULTS

Our experimental set-up comprises a *T*-junction droplet generator and an outlet channel that bifurcates into two branches of—within the experimental resolution—equal length made by soft lithography [28]. These branches reconnect downstream, as depicted in Fig. 1(a). The channels were 100 μm wide and 50 μm tall, and the length of each branch was $l=3.25$ mm. The continuous phase was hexadecane with 3% Span80 surfactant (viscosity $\mu_c \sim 8$ mPa s) and the dispersed phase an aqueous solution of black ink (viscosity $\mu_d \sim 1$ mPa s). The droplets were formed upstream of the loop and we varied the frequency at which the droplets entered the bifurcation by changing the rates of flow of the two immiscible phases. We chose the flow conditions so (i) that the droplets are slightly larger than the capillary size and therefore form small plugs, as can be seen in Fig. 1(a), and (ii) that the drops do not break up at the bifurcation [3]. We varied the frequency (f) at which the droplets arrived at the bifurcation by changing the rates of flow of the two phases. In particular, increasing the rate of flow of the discontinuous phase increased the frequency of drop formation. This was accompanied by a small but systematic increase in the size of the drops.

As the drops arrived at the bifurcation, they did not break but flowed into one of the two branches, as previously observed by Link *et al.* [3]. We observed that the droplets systematically flowed into the branch containing the smaller number of drops. This is consistent with the following assumptions, which we will detail in the remainder of the paper: (i) droplets go to the arm, where the inflow of continuous phase is greater [29], and (ii) each droplet slows down the flow of the arm it is in by adding some viscous resistance. Since the droplets added resistance to flow [5,6] they affected the resistances of the channels and modified the decisions undertaken by subsequent droplets. The sequence of left/right choices depended on the ratio of the frequency of feeding (f) to the frequency associated with the time it took for the droplets to travel through the loop ($\sim l/u$, where u is the mean speed of flow of the continuous fluid through any of the two arms). Figures 1(b)–1(d) show three representative sequences. At low frequency [Fig. 1(b)], all droplets chose the right branch. Each droplet left the loop before the next one entered it, so that each choice depended only on the static parameters of network, and the small imbalance in the lengths of the two arms resulted in the uniform preference for the right branch. As we increased the frequency, drops arrived at the bifurcation while previous ones were still in

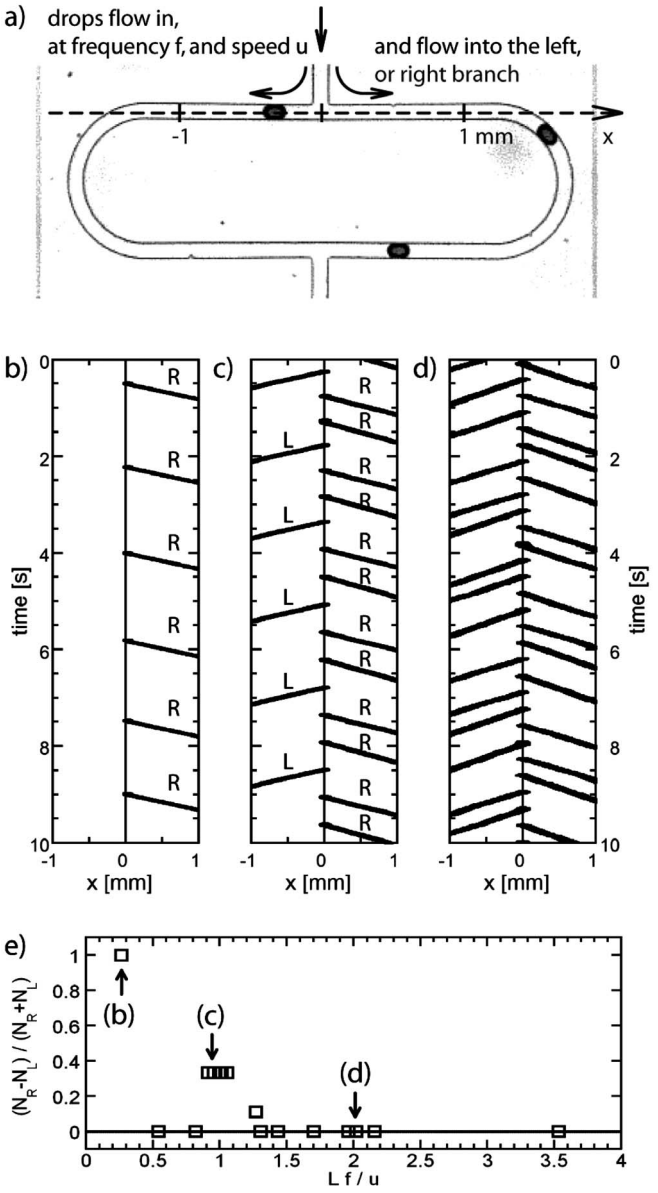

FIG. 1. (a) A micrograph of the experimental setup. The dashed line marks the axis along which we measured the positions of the droplets. (b), (c), (d) space-time diagrams of the trajectories of the droplets traveling through the single microfluidic loop, fed into the loop at 0.59, 1.81, and 2.93 Hz and 7.27, 5.91, and 4.72 mm/s, respectively. (e) a graph of the mean ratio of the numbers of droplets traveling through each of the two arms of the loops, plotted as a function of the nondimensionalized frequency of feeding.

the loop. Under these conditions the choice of the trajectory was dictated by the dynamically changing resistances of the two arms. An example of a periodic sequence of trajectories is shown in Fig. 1(c) while Fig. 1(d) exemplifies an irregular pattern of flow. Notably, the imbalance in the number of droplets choosing the right over the left branch is far greater than the (small) imbalance of the resistances of the arms of the loop. For example, at low frequency all drops traveled through the right arm and $(n_R-n_L)/(n_R+n_L)=1$, [Fig. 1(a)]. In Fig. 1(e) we plotted the imbalance as a function of the

nondimensional frequency (lf/u) of feeding; this plot shows a pronounced peak at $lf/u \sim 1$.

We constructed a simple model to recover this behavior numerically. In a first approximation the laminar flow of a fluid in a channel with constant cross section can be described via the relationship between pressure drop Δp and flow rate q, via the hydrodynamic resistance to flow r

$$\Delta p = rq. \tag{1}$$

For multiphase systems, the resistance depends on the composition of the fluid within the channel. For liquid-liquid flows of droplets of a size larger than that of the channel and for complete dewetting of the dispersed phase from the channel wall, the pressure drop will stem from viscous dissipation in the bulk phases (both in the continuous and the dispersed fluids) and from the recirculation of the flow of the continuous fluid at the tips of the immiscible slugs [6,7]

$$r_{eff} = 12.8\frac{l}{b^3 w}\mu(\lambda\phi + 1 - \phi) + n_d \times 3.15 g(\lambda)\frac{\gamma}{b}\frac{\mathrm{Ca}^{2/3}}{q}, \tag{2}$$

where γ is the surface tension, μ is the continuous phase viscosity, Ca is the capillary number $\mathrm{Ca} = \mu u/\gamma$, λ is the ratio of dispersed to continuous phase viscosity, and $g(\lambda)$ depends on viscosity ratio [7].

The first term of Eq. (2) is the viscous resistance associated with the flow in the plugs of dispersed phase and in the continuous phase between the plugs, where l is the channel length, b its smallest cross dimension (height) w its width, μ is the viscosity of the continuous phase, and ϕ is the volume fraction of dispersed phase, with a numerical prefactor corresponding to the flow in a rectangular channel with aspect ratio $w/b=2$ [25]. While the first term depends on the volume fraction of the two phases, the second term is a function of the number of droplets in the channel n_d, and the capillary number $\mathrm{Ca} = \mu u/\gamma$, where u is the average speed of flow. It was first derived by Bretherton for gas bubbles in circular capillaries [5] and extended to viscous fluids and soft solid inclusions [6,7] for the limiting case $\mathrm{Ca} \ll 1$. In Eq. (2) we use the prefactor 3.15 determined for a rectangular channel with aspect ratio 2 by Wong *et al.* [6]. Equation (2) contains a dependence on viscosity ratio indicated as a prefactor $g(\lambda)$. Hodges *et al.* have shown that the film thickness around a viscous plug in a circular capillary has only a weak dependence on viscosity ratio, with $g(\lambda)$ varying between 1 and ~ 1.5 between $\lambda = 0$ and ∞ [7]. Similarly we expect that $g(\lambda)$ will have a small effect and will not change qualitatively the behavior expected from Eq. (2).

In a recent publication we have investigated the behavior of multiphase flows in microchannels within an "averaged" approximation, where effective channel resistance due to droplets contained in channel is reduced to the effect of the volume fraction of the dispersed phase [30]. This approximation reduces Eq. (2) to its first term, neglecting the fact that dispersed phase is present as separate drops. Very recently, Engl *et al.* [9] have also studied the dynamics of droplets at a capillary bifurcation, and analyzed the resistance with a model similar to the first term of Eq. (2). Because they were using a dispersed phase of viscous oil in water, droplets increased the pressure drop in the branch in which they traveled, and hence decreased the flow rate in this branch, thereby increasing the tendency for the next droplet to choose the alternate branch. Limiting the approximation of channel resistance to the first term of Eq. (2) would not correctly represent the experiments described here, where the dispersed phase is less viscous than the continuous phase. The postulate we employ in the second term of (2), i.e., that the added resistance of the droplets does not depend on their length, stems from the fact that the dominant contribution to the added dissipation associated with the presence of a drop in the channel arises from the recirculation of the continuous fluid around the front and back of the droplet [5].

Our simple model reproduces qualitatively the experimental observations. In the following, capital letters denote nondimensional quantities and lower-case letters denote dimensional ones. The system consists of a single inlet channel through which the flow travels with constant velocity u. The channel splits at a bifurcation point into 2 arms that diverge to the left and right. For completeness, we consider the possibility of different lengths of the arms of the loop. Because we look at a train of droplets arriving at regular intervals, the system is made nondimensional by the droplet frequency f and the average velocity u. The unit length thus becomes $l_0 = u/f$. Each arm of the loop has the same cross section but may have different lengths, so that their resistance is directly characterized by their length, respectively l_L and l_R. The average flow velocity in the arms u_L and u_R satisfy the following relations:

$$u_L + u_R = u, \tag{3}$$

$$\frac{u_L}{u_R} = \frac{r_R(l_R, n_R)}{r_L(l_L, n_L)}. \tag{4}$$

The latter equation assumes that the pressure drop in the arms of the loop is dominated by viscous dissipation, as expected at low Re. For channels of equal cross section, the resistance is simply given by the channel length and the number of drops per channel. When no drops are present $u_L/u_R = l_R/l_L$. As we do not measure pressure, we only need to know the relative resistance of each channel with respect to the other to know the velocities and therefore can use a-dimensional resistances, defined with respect to the unit length l_0, and denoted by a capital letter R. We assume that each droplet changes the resistance of a channel by a fixed amount R_d. For example, the resistance of the left channel is

$$R_L = \frac{l_L}{l_0} + n_L \times R_d. \tag{5}$$

In (5) we neglect the physical size of the droplets. This is equivalent to assuming that droplets occupy a small volume fraction, so that the change of value of the first term in Eq. (2) associated with the presence of droplet remains small. Equation (2) also suggests that the added droplet resistance R_d should depend on velocity as $u^{-1/3}$. As this dependence is small, and the average velocity only varies slightly in experiments, we neglect this dependence and use instead the aver-

age capillary number of the flow unperturbed by drops. For small volume fraction $\phi \ll 1$ and small viscosity ratio $\lambda \ll 1 R_d$ becomes

$$R_d \approx 0.25\left(\frac{bf}{u}\right)\mathrm{Ca}^{-1/3}. \quad (6)$$

This equation is obtained by nondimensionalizing Eq. (2) in the form of Eq. (5). The nondimensionalization makes apparent that there are only 3 independent variables (within the chosen approximations) in this setup, which we chose in the model as follows: the nondimensional frequency $l_L f/u$ of inserting the droplets into the loop; the ratio of channel length l_R/l_L, and the droplet resistance R_d. In the experiments both channels have the same length l. Typical values used for the experiment with $lf/u \sim 1$ are: channel depth $b=50$ μm, speed of flow $u=0.31$ cm/s, viscosity $\mu=8$ mPa s, surface tension $\gamma=6$ mN/m and frequency $f=1.81$ Hz, yielding $R_d \sim 0.02$. While this value represents the current experimental setup, R_d can vary widely in other circumstances and indeed changes with the frequency of droplet arrival as well as the speed of flow. Our aim, however, is to identify the key features and controlling parameters of the experimental system, rather than an exact description. Therefore we chose to run the simulations with a constant value of R_d, regardless of the other parameters. We probe the behavior of the system over a range of values of R_d from 0 to 0.5.

We start the simulation by choosing the (a-dimensional) lengths of the two arms of the loop L_R and L_L. We then send successive droplets at regular intervals $t=1,2,\ldots$ into the bifurcation. Each droplet flows into the arm characterized by lower resistance. We count the number of drops in each channel to determine its resistance, and to calculate the speed of flow. The simulation is then advanced to the next event which changes the number of drops in the channels—that is, either a droplet entering or leaving the loop. The whole procedure is then reiterated. We record a series of droplet bifurcation events as a list $\{C_i\}$ of where the ith droplet has gone. To establish a long time regime we only count the events between $i=100$ and $i=124$. We then look for the minimum repeating sequence within this series. This procedure avoids double counting of sequences such as $\{RL\}$ and $\{LR\}$ as distinct flow patterns. In order to visualize the behavior of the system in the space spanned by the lengths of the two arms, we transformed the sequences $\{C_i\}$ into a 12-bit color coding by putting $L=0$ and $R=1$ [in this procedure, sequences shorter than 12 bits were repeated to form the full (12 bit) code of the color, and sequences longer than 12 bits were truncated; a single color therefore may correspond to several series larger than 12 bits]. The simulation is then repeated for another pair of channel length, until a complete map $L_{R,min} < L_R < L_{R,max}$ and $L_{L,min} < L_L < L_{L,max}$ is built.

Figure 2 presents the complexity of flow patterns produced by our model. We vary the channel length between 0.5 and 3 for various values of the droplet resistance $R_d=0.1$ [Fig. 2(a)] and 0.5 [Fig. 2(b)]. Far from the diagonal ($L_L=L_R$) all droplets go either to the left or to the right, as the presence of the droplets is not enough to increase the resistance of the shorter branch sufficiently to divert the drops to the longer one. Closer to the diagonal, however, we observe complex color maps showing a wide variety of possible series. The complexity increases with increasing length of the arms (and thus with decreasing relative resistance introduced by the individual drops). Importantly, we identify regions of apparently chaotic dynamics where small changes in parameters lead to a wide variety of different series.

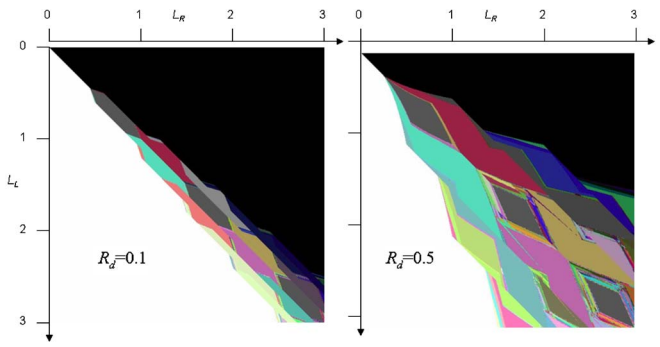

FIG. 2. (Color online) Maps of the (L/R) bifurcation sequences for drop arriving at a T junction. Each point in the map represents a sequence of 12 successive bifurcation events. The sequences are transformed into a color by using the 4 first digits to code for red, the next 4 to code for blue, and the last 4 to code for green. Each map is constructed from an exhaustive analysis of 500 $R_L \times 500 R_R$ sequences.

Close to the diagonal, we note large and regular quadrangular "grey" regions signaling simple $\{RL\}$ series. These are expected, as the diagonal corresponds to equal channel length and resistance. These regions are, however, separated by colored regions, which show a multitude of adjacent sequences.

We compare our numerical results to experiment by plotting the imbalance of the number of drops traveling in each

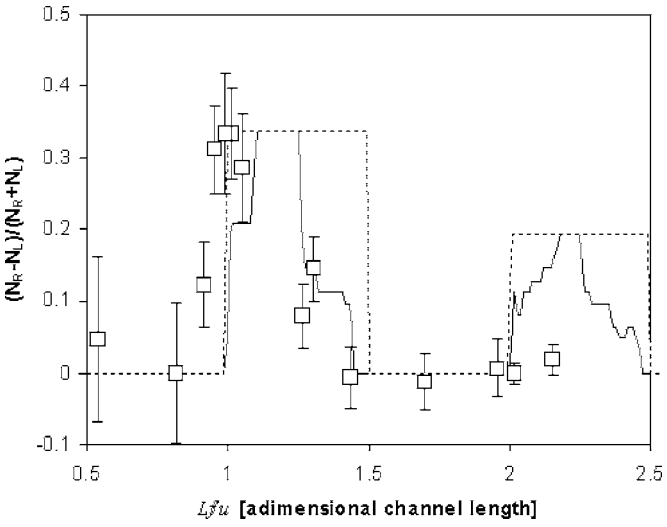

FIG. 3. Difference between the number of droplets going right and left at a T junction with both branches of almost equal length, depending on the added droplet resistance R_d. For equal flow velocity, we assume that a droplet will preferentially go right. Solid line: theoretical curve for $R_d=0.1$; dashed line: theoretical curve for $R_d \to 0$. Points are experimental observations.

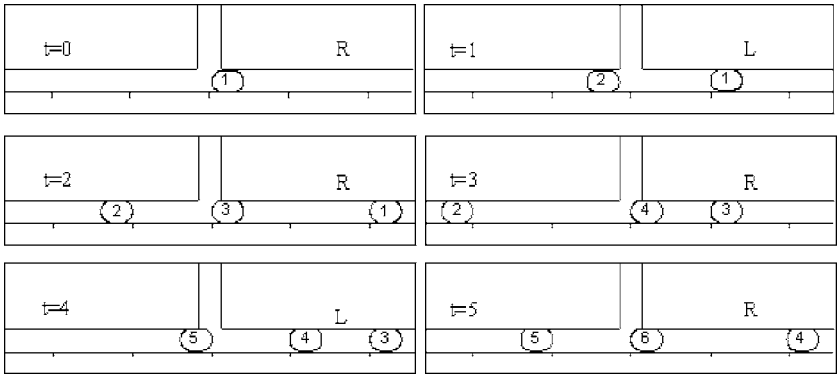

FIG. 4. Behavior of droplet at a bifurcation in the limiting case of $L_R=L_L=1.25$, $R_d=0$.

of the two arms of almost equal length. In agreement with the experimental observations, we find (Fig. 3) that in between the grey regions, substantially more droplets enter the right channel than the left one. This imbalance is stronger for smaller R_d and smaller channel length, and reaches up to 2 drops in the right channel to 1 in the left. It is caused by the infinitesimal preference for the right channel hard wired in the model, and can be understood in the limiting case as depicted in Fig. 4. This limiting case corresponding to $R_d \to 0$ (but still larger than the intrinsic preference for the right channel hardwired in the model) illustrates the system's behavior. Consider, for example, a system with channel length slightly longer than 1, as sketched in Fig. 4. As the additional resistance introduced by the droplet is virtually negligibly small and both branches have the same length, velocity of the flow in each branch is $\sim 1/2$. Each droplet is introduced at integral time $t=0,1,2,\ldots$. At $t=0$, the first drop goes right due to the imposed preference. At $t=1$, the next drop goes left because the right branch already contains a drop. At $t=2$, the next drop goes right because there is 1 drop in each branch and of the imposed preference. At $t=3$ the drop goes again to the right because one drop has moved out of the tube to the right, but not out of the one to the left so again there are the same number of drops in each tube. The next drop ($t=4$) goes left because there are two drops in the right channel and none in the left channel. The situation at $t=5$ then reproduces $t=2$ so that 2/3 of the total number of drops go right while only 1/3 go left. An infinitesimal preference for one of the channels clearly suffices to induce this imbalance. This small, initial imbalance may derive from, e.g., small differences in the lengths or cross sections of the downstream capillaries, and leads to the complex, chaotic behavior noted earlier in both experiments and simulations.

III. CONCLUSIONS

We report the patterns of flow of individual droplets through the simplest network possible—a single loop. Our results demonstrate that the patterns of flow can be both periodic and irregular, depending on the ratio of the frequency at which they are fed into the loop to the frequency associated with the mean time needed for any drop to travel through the loop. The results of the simulations show that the density of the number of distinct sequences of trajectories varies substantially as the ratio of the lengths of the arms of the loop and the ratio of the added resistance of the drops to the resistance of the channels are varied. Moreover, the amplification of the slightest imbalance of the resistances of the two arms results in a large imbalance in the number of drops traveling through each branch. These observations prompt several questions concerning the patterns of flow of droplets through more complicated networks: Over what range of parameters are these flows regular or chaotic? What is the load of the nodes in complicated networks? As the interconnectivity of the network is increased, is this load distributed evenly between the branches, or are there strong imbalances? Can these imbalances be predicted? These questions are not only interesting from the point of view of physics (as flows of discrete 'resistors' through networks) but are also relevant to the design of lab-on-chip devices operating on droplets [12], and parallelization of microfluidic techniques in general (e.g., emulsification). The result that there exist ranges of the parameters governing the behavior of the system which promote regular dynamics suggests that, with appropriate care, it should be possible to design networks of channels that will promote desired (e.g., for multiplexing) sequences of trajectories of the droplets with the use of the "passive" response of the system, and without the need for active manipulation of the trajectories of individual droplets.

ACKNOWLEDGMENTS

P.G. thanks the Foundation for Polish Science for financial support. Some of the experimental work was carried out at Harvard University by M.J.F., and was supported by US Department of Energy Grant No. DE-FG02-OOER45852.

[1] H. A. Stone, A. D. Stroock, and A. Ajdari, Annu. Rev. Fluid Mech. **36**, 381 (2004).
[2] S. L. Anna, N. Bontoux, and H. A. Stone, Appl. Phys. Lett. **82**, 364 (2003).
[3] D. R. Link, S. L. Anna, D. A. Weitz, and H. A. Stone, Phys. Rev. Lett. **92**, 054503 (2004).
[4] P. Garstecki, M. Fuerstman, H. A. Stone, and G. M. Whitesides, Lab Chip **6**, 437 (2006).
[5] F. P. Bretherton, J. Fluid Mech. **10**, 166 (1961).
[6] H. Wong, C. J. Radke, and S. Morris, J. Fluid Mech. **292**, 95 (1995).
[7] S. R. Hodges, O. E. Jensen, and J. M. Rallison, J. Fluid Mech. **501**, 279 (2004).
[8] P. Garstecki, M. A. Fischbach, and G. M. Whitesides, Appl. Phys. Lett. **86**, 244108 (2005).
[9] W. Engl, M. Roche, A. Colin, P. Panizza, and A. Ajdari, Phys. Rev. Lett. **95**, 208304 (2005).
[10] M. W. Losey, M. A. Schmidt, and K. F. Jensen, Ind. Eng. Chem. Res. **40**, 2555 (2001).
[11] S. Ilya, D. T. Joshua, and R. F. Ismagilov, Lab Chip **4**, 316 (2004).
[12] M. Joanicot and A. Ajdari, Science **309**, 887 (2005).
[13] M. B. Furman and W. L. Olbricht, Biotechnol. Prog. **1**(1), 26-32 (1985).
[14] R. T. Carr and M. Lacoin, Ann. Biomed. Eng. **28**, 641 (2000).
[15] R. T. Carr, J. B. Geddes, and F. Wu, Ann. Biomed. Eng. **33**(6), 764 (2005).
[16] M. J. Blunt, Curr. Opin. Colloid Interface Sci. **6**, 197 (2001).
[17] M. J. Blunt, M. D. Jackson, M. Piri, and P. H. Valtvane, Adv. Water Resour. **25**, 1069 (2002).
[18] E. Yildiz, B. Keskinler, T. Pekdemir, G. Akay, and A. Nuhoglu, Chem. Eng. Sci. **60**, 1103 (2005).
[19] G. Keramas, G. Perozziello, O. Geschke, and C. B. V. Christensen, Lab Chip **4**, 152 (2004).
[20] Q. F. Xue, A. Wainright, S. Gangakhedkar, and I. Gibbons, Electrophoresis **22**, 4000 (2001).
[21] R. L. Chien and J. W. Parce, Fresenius' J. Anal. Chem. **371**, 106 (2001).
[22] A. Grodrian, J. Metze, T. Henkel, K. Martin, M. Roth, and J. M. Kohler, Biosens. Bioelectron. **19**, 1421 (2004).
[23] J. W. Hong, V. Studer, G. Hang, W. F. Anderson, and S. R. Quake, Nat. Biotechnol. **22**, 435 (2004).
[24] T. Thorsen, S. J. Maerkl, and S. R. Quake, Science **298**, 580 (2002).
[25] P. Tabeling, *Introduction à la microfluidique* (Belin, Paris, 2003).
[26] J. Zeng and T. Korsmeyer, Lab Chip **4**, 265 (2004).
[27] M. K. Runyon, B. L. Johnson-Kerner, and R. F. Ismagilov, Angew. Chem., Int. Ed. **43**, 1531 (2004).
[28] G. M. Whitesides and A. D. Stroock, Phys. Today **54**, 42 (2001).
[29] M. DeMenech, Phys. Rev. E **73**, 031505 (2006).
[30] F. Jousse, G. Lian, R. Janes, and J. Melrose, Lab Chip **5**, 646 (2005).